Research Article Vol. 37, No. 5 / May 2020 / Journal of the Optical Society of America A 859

Journal of the Optical Society of America A

OPTICS, IMAGE SCIENCE, AND VISION

Propagation of time-resolved fluorescence in a diffuse medium: complex analytical derivation

Anand T. N. Kumar

Department of Radiology, Massachusetts General Hospital, Harvard Medical School, Charlestown, Massachusetts 02129, USA (ankumar@nmr.mgh.harvard.edu)

Received 23 January 2020; revised 6 April 2020; accepted 6 April 2020; posted 7 April 2020 (Doc. ID 388762); published 29 April 2020

The spatiotemporal evolution of fluorescence in an optically diffusive medium following ultrashort laser pulse excitation is evaluated using complex analytical methods. When expressed as a Fourier integral, the integrand of the time-resolved diffuse fluorescence with embedded fluorophores is shown to exhibit branch points and simple pole singularities in the lower-half complex-frequency plane. Applying Cauchy's integral theorem to solve the Fourier integral, we calculate the time-resolved signal for fluorescence lifetimes that are both shorter and longer compared to the intrinsic absorption timescale of the medium. These expressions are derived for sources and detectors that are in the form of localized points and wide-field harmonic spatial patterns. The accuracy of the expressions derived from complex analysis is validated against the numerically computed, full time-resolved fluorescence signal. The complex analysis shows that the branch points and simple poles contribute to two physically distinct terms in the net fluorescence signal. While the branch points result in a diffusive term that exhibits spatial broadening (corresponding to a narrowing with time in the spatial Fourier domain), the simple poles lead to fluorescence decay terms with spatial/spatial-frequency distributions that are independent of time. This distinct spatiotemporal behavior between the diffuse and fluorescence signals forms the basis for direct measurement of lifetimes shorter than the intrinsic optical diffusion timescales in a turbid medium.

https://doi.org/10.1364/JOSAA.388762

1. INTRODUCTION

It is well known that the spatial distribution of a short laser pulse (∼ femtoseconds to picoseconds) of near-infrared light traversing a turbid medium exhibits a time-dependent spatial variance [1,2]. This process can be understood using the diffusion or transport equations for light propagation in turbid media [3]. In the spatial-frequency domain (SFD), which is the Fourier transform of coordinate space, this spatial broadening corresponds to a narrowing of the distribution of the diffuse fluorescence signal in time. As a consequence, it has been recognized that high spatial frequencies attenuate more rapidly than lower spatial frequencies [4]. This observation is a time-domain (TD) generalization of the well-known fact [5] that the diffuse medium acts as a spatial low-pass filter by rejecting high-frequency components.

The use of SFD excitation and detection has been explored for biomedical applications, using both steady state and pulsed laser excitation [5–10]. We have previously shown experimentally that high spatial frequencies allow direct measurement of intrinsic fluorescence lifetimes from thick turbid tissue [11]. Here, we present a theoretical study of the spatiotemporal behavior of pulsed laser excitation in a medium embedded with fluorescent dyes, using methods of complex integration. Using contour integration, we derive an expression for the entire time resolved fluorescence signal for arbitrary lifetimes and for both point sources and harmonic spatial illumination and detection. The accuracy of these results is validated against the numerically computed exact time-resolved fluorescence signal in a diffuse medium. The results show a clear delineation of time-resolved fluorescence into a diffuse and fluorescent component with distinct spatiotemporal behavior. In the SFD, the temporal decay rate of the diffuse term increases with spatial frequency, analogous to the temporal propagation of intrinsic diffuse light. However, the decay of the fluorescence term is independent of spatial frequency or optical properties but reflects the characteristic lifetime of the fluorophore in the tissue environment. The fluorescence signal therefore remains significant at high spatial frequencies and long times, where the diffuse term is rapidly eliminated, thereby enabling direct measurement (without tomographic inversion) of intrinsic fluorescence lifetimes within a turbid medium that are comparable to or even shorter than the intrinsic diffusion timescales.

2. THEORY

In general, diffuse fluorescence could arise from an arbitrary distribution of fluorophore(s) within a turbid medium. We consider a uniform turbid medium, characterized by homogeneous optical absorption, $\mu_a^{x,m}$, and reduced scattering coefficient,

$\mu_s'^{x,m}$, at wavelengths λ_x and λ_m. Suppose that the medium consists of N fluorophores with distinct lifetimes, described by yield distributions $\eta_j(\mathbf{r}) = \epsilon_j n_j(\mathbf{r}) Q_j$ [where $n_j(\mathbf{r})$ is the concentration distribution, ϵ_j is the extinction coefficient, and Q_j is the emission quantum yield] and corresponding fluorescence lifetimes $\tau_j = 1/\Gamma_j$, $j = 1:N$. Assuming that a single absorption/emission event adequately describes the generation of fluorescence (a condition well satisfied given the wide separation of typical fluorophore absorption and emission spectra), the detected fluorescence intensity at a location $\mathbf{r}_d$ (such as a fiber tip or camera pixel) on the medium boundary, at time t, due to excitation by a point source at $\mathbf{r}_s$ at time $t = 0$ can be written as a Fourier integral (omitting experimental scaling factors for simplicity):

$$U_F(\mathbf{r}_s, \mathbf{r}_d, t) = \frac{1}{2\pi} \int_{-\infty}^{\infty} d\omega e^{-i\omega t} \int_{\Omega} d^3 r \times W(\mathbf{r}_s, \mathbf{r}_d, \mathbf{r}, \omega) \left[\sum_n \frac{i\eta_n(\mathbf{r})}{\omega + i\Gamma_n} \right], \quad (1)$$

where

$$W(\mathbf{r}_s, \mathbf{r}_d, \mathbf{r}, \omega) = \mathcal{G}^x(\mathbf{r}_s, \mathbf{r}, \omega) \mathcal{G}^m(\mathbf{r}_d, \mathbf{r}, \omega) \quad (2)$$

is the frequency domain (FD) weight function, also called the sensitivity function, with $\mathcal{G}^{x,m}$ representing the Green's functions of the FD diffusion equations for wavelengths λ_x and λ_m. To solve Eq. (1), we examine the behavior of the integrand of Eq. (1) (which corresponds to the expression for FD diffuse fluorescence [12]) in the complex-frequency plane [13]. It is immediately clear that the quantity in square brackets in the integrand of Eq. (1) [which is the Fourier transform of the exponential decay, $exp(-t/\tau)$] results in simple pole singularities in the negative imaginary axis, located at $\omega = -i\Gamma_n$. The sensitivity function W exhibits a non-trivial structure in the complex plane due to the diffuse Green's functions $\mathcal{G}^{x,m}$. To see this, we consider the case of an unbounded homogeneous medium. The corresponding Green's functions are

$$\mathcal{G}_0^{x,m}(\mathbf{r}_1, \mathbf{r}_2, \omega) = \exp(ik_{x,m}|\mathbf{r}_1 - \mathbf{r}_2|)/4\pi D_{x,m}|\mathbf{r}_1 - \mathbf{r}_2|, \quad (3)$$

with

$$k_{x,m} = \sqrt{\frac{(-v\mu_a^{x,m} + i\omega)}{D_{x,m}}}, \quad (4)$$

where $D^{x,m} = v/3\mu_s'^{(x,m)}$ is the diffusion coefficient [14], and v is the velocity of light in the medium. Note that the homogeneous Green's functions are dependent only on the magnitude of the difference between the coordinates $|\mathbf{r}_s - \mathbf{r}|$ and $|\mathbf{r} - \mathbf{r}_d|$ and not on their absolute values. It is evident from Eqs. (3) and (4) that the homogeneous Green's function is bivalued owing to the square root in k. This implies branch points [13] in the complex plane structure, along the negative imaginary axis at $\omega = -iv\mu_a^{x,m}$ (Fig. 1). (It is interesting to compare the complex plane structure in Fig. 1 to that for linear dispersive electromagnetic pulse propagation in dielectric media [15].)

Armed with the full complex plane structure of the integrand in Eq. (1), we can now use Cauchy's integral theorem [13] to solve the integral. We first draw a branch cut along the negative imaginary axis from $-\min(v\mu_a^{x,m})$ to $-\infty$. We choose a contour, shown in Fig. 1, that encircles the simple poles in the lower-half plane while avoiding crossing the branch cut along the negative imaginary axis. The contour consists of three parts: the line integral along the real ω axis, sections of a semicircle in the lower-half plane, and two line integrals on the negative imaginary axis on either side of the branch cut. Two distinct scenarios arise, depending on the value of the decay rate Γ_n relative to the timescale, $\tau_a = 1/v\mu_a^{x,m}$, which is the asymptotic decay constant of intrinsic time-resolved diffuse light and is related solely to the absorption coefficient [1]. When $\tau_n > \tau_a$, i.e., $\Gamma_n < 1/\tau_a$, the simple pole at $-i\Gamma_n$ is outside the branch cut. The contour integral then results in a residue when Cauchy's theorem is applied to the entire closed contour, while the integrals along the branch cut result in a non-zero contribution from either side of the branch points. When $\tau_n < \tau_a$, or $\Gamma_n > 1/\tau_a$, the simple pole rests on the branch cut, and integrals along the branch cuts now include semi-circles surrounding the poles, resulting in a residue (at $-i\Gamma_n$) and a principal value integral. The contributions to each portion of the contour are evaluated using standard methods [13].

The final result is that the net fluorescence signal separates into two parts, the first corresponding to spatiotemporally spreading terms (arising from integration around the branch points) and the other corresponding to pure fluorescence decay terms (arising from the residues at the simple poles) with exponential time dependence dictated by the fluorescence lifetimes:

$$U_F(\mathbf{r}_s, \mathbf{r}_d, t) = \sum_n [a_{Dn}(\mathbf{r}_s, \mathbf{r}_d, t) + a_{Fn}(\mathbf{r}_s, \mathbf{r}_d)], \quad (5)$$

where a_{Fn} is the fluorescence decay amplitude of the n'th lifetime and is given as the residue of the weight function W at $\omega = -i\Gamma_n$:

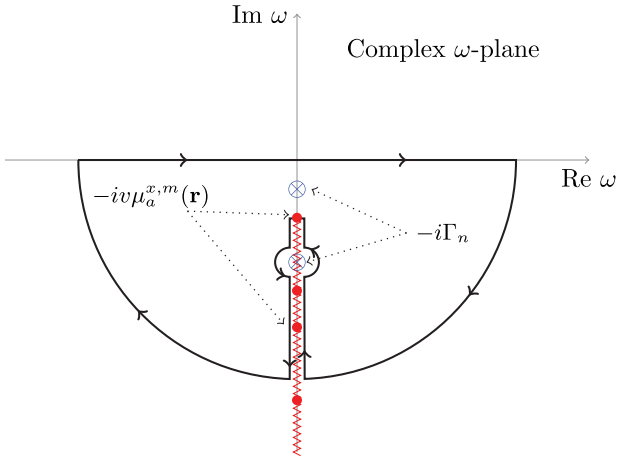

Fig. 1. Complex plane structure for the frequency domain diffuse fluorescence [integrand of Eq. (1) in the text] showing simple pole singularities at $-i\Gamma_n$ (⊗) corresponding to fluorescence decays with lifetimes $\tau_n = 1/\Gamma_n$, and branch points at $-iv\mu_a^{(x,m)}$ (red filled circle) arising from the diffusion Green's functions. The zig-zag line shows the branch cut extending along the negative imaginary axis from the smallest value of $v\mu_a^{x,m}(\mathbf{r})$ to $-\infty$.

$$a_{Fn} = e^{-\Gamma_n t} \int_\Omega \mathrm{d}^3 r \eta_n(\mathbf{r}) \begin{cases} W(\mathbf{r}_s, \mathbf{r}_d, \mathbf{r}, -i\Gamma_n), & \text{if } [\Gamma_n < v\mu_a] \\ \mathcal{R}e\,[W(\mathbf{r}_s, \mathbf{r}_d, \mathbf{r}, -i\Gamma_n)] & \text{if } [\Gamma_n > v\mu_a] \end{cases}, \tag{6}$$

and a_{Dn} is the diffusive term arising from the integrals around the branch cuts:

$$a_{Dn} = -\int_\Omega \mathrm{d}^3 r \eta_n(\mathbf{r}) \begin{cases} I(\mathbf{r}_s, \mathbf{r}_d, \mathbf{r}, t), & \text{if } [\Gamma_n < v\mu_a] \\ \mathcal{P}\,[I(\mathbf{r}_s, \mathbf{r}_d, \mathbf{r}, t)] & \text{if } [\Gamma_n > v\mu_a] \end{cases}, \tag{7}$$

where I denotes the integrals along the branch cut:

$$I = \frac{1}{\pi} \int_{v\mu_a}^{\infty} \mathrm{d}\gamma \frac{\mathcal{I}m\,[W(\mathbf{r}_s, \mathbf{r}_d, \mathbf{r}, -i\gamma)]}{\gamma - \Gamma_n} e^{-\gamma t}, \tag{8}$$

with $\mathcal{P}$ denoting the Cauchy principal value, and $\mathcal{R}e$, $\mathcal{I}m$ refer to real and imaginary parts, respectively. The Cauchy principal value integral is evaluated around the singularity at $\gamma = \Gamma_n$. Although we have assumed an infinite homogeneous medium in the derivation above, it is plausible to expect that the complex plane structure in Fig. 1 is maintained for arbitrary bounded and non-uniform media, where the lower imaginary axis will now be populated with multiple branch points corresponding to the values of $\mu_a^{x,m}(\mathbf{r})$ throughout the medium [In the case of a heterogeneous medium, the lowest absorption needs to be used as the starting point of the branch cut in Fig. 1]. Thus, we expect the key result, namely, the temporal separation of diffuse and fluorescence contributions, to be of more general validity. Indeed, the expression for a_{Fn} in Eq. (6) for the case of $\Gamma_n < v\mu_a$ is identical to that derived previously [16] using the radiative transport for arbitrary heterogeneous media. Note that both a_{Dn} and a_{Fn} depend on the FD sensitivity matrices $W(\mathbf{r}_s, \mathbf{r}_d, \mathbf{r}, \omega)$ evaluated at an imaginary frequency of $\omega = -i\Gamma_n$ or $-i\gamma$, respectively. Using these values of ω in the definition of $k_{x,m}$ in Eq. (4), it is clear that an imaginary frequency reduces the FD weight function into a steady state or continuous-wave (CW) weight function but with an altered absorption coefficient. Thus, a_F depends on the CW weight functions evaluated at a reduced absorption of $\mu_a - \Gamma_n/v$, $\forall \Gamma_n$ (which is negative when $\Gamma_n > v\mu_a$, i.e., when the lifetimes are shorter than the absorption timescale), while a_D depends on the CW Green's function evaluated at a negative absorption of $\mu_a - \gamma_n/v$. Thus, the entire TD fluorescence signal is expressed in terms of the CW, i.e., steady state Green's functions and their analytic continuation to negative absorption.

We now write the above results in SFD, where the point sources and detectors ($\mathbf{r}_s$ and $\mathbf{r}_d$) are replaced by wide-field, sinusoidal spatial patterns with frequencies ($\mathbf{k}_s$, $\mathbf{k}_d$). The measured fluorescence signal in SFD from Eq. (1) is a direct Fourier transform with respect to the spatial coordinates $\mathbf{r}_s$ and $\mathbf{r}_d$:

$$\tilde{U}_F(\mathbf{k}_s, \mathbf{k}_d, t) = \int \mathrm{d}^3\mathbf{r}_s \int \mathrm{d}^3\mathbf{r}_d e^{i(\mathbf{k}_s \cdot \mathbf{r}_s + \mathbf{k}_d \cdot \mathbf{r}_d)} U_F(\mathbf{r}_d, \mathbf{r}_s, t). \tag{9}$$

We then get, analogous to Eq. (5),

$$\tilde{U}_F(\mathbf{k}_s, \mathbf{k}_d, t) = \sum_n \left[\tilde{a}_{Dn}(\mathbf{k}_s, \mathbf{k}_d, t) + \tilde{a}_{Fn}(\mathbf{k}_s, \mathbf{k}_d)\right], \tag{10}$$

where $\tilde{a}_{Dn}$ and $\tilde{a}_{Fn}$ are the spatial Fourier transforms of a_{Dn} and a_{Fn}, expressed as

$$\tilde{a}_{Fn} = e^{-\Gamma_n t} \int_\Omega \mathrm{d}^3 r \eta_n(\mathbf{r}) \begin{cases} \tilde{W}(\mathbf{k}_s, \mathbf{k}_d, \mathbf{r}, -i\Gamma_n), & \text{if } [\Gamma_n < v\mu_a] \\ \mathcal{R}e\left[\tilde{W}(\mathbf{k}_s, \mathbf{k}_d, \mathbf{r}, -i\Gamma_n)\right] & \text{if } [\Gamma_n > v\mu_a] \end{cases} \tag{11}$$

and

$$\tilde{a}_{Dn} = -\int_\Omega \mathrm{d}^3 r \eta_n(\mathbf{r}) \begin{cases} \tilde{I}(\mathbf{k}_s, \mathbf{k}_d, \mathbf{r}, t), & \text{if } [\Gamma_n < v\mu_a] \\ \mathcal{P}\left[\tilde{I}(\mathbf{k}_s, \mathbf{k}_d, \mathbf{r}, t)\right] & \text{if } [\Gamma_n > v\mu_a] \end{cases}, \tag{12}$$

where $\tilde{I}$ is obtained from Eq. (8) by replacing $W(\mathbf{r}_s, \mathbf{r}_d, \mathbf{r}, -i\gamma)$ with its spatial Fourier transform, $\tilde{W}(\mathbf{k}_s, \mathbf{k}_d, \mathbf{r}, -i\gamma)$.

Equations (5)–(8) and the corresponding SFD expressions Eqs. (10)–(12) constitute the central results of this paper, and express the time-resolved fluorescence propagation within a diffuse medium entirely in terms of analytically continued steady state Green's functions evaluated at reduced or negative absorption. These expressions are valid for arbitrary fluorescence lifetimes and fluorophore distributions. The key result is the separation of the total fluorescence signal from a diffuse medium into a diffusive component, which exhibits a time-dependent spatial (or spatial frequency) distribution, and a purely fluorescent decay term, which exhibits a time dependence dictated by the pure exponential decay of the intrinsic fluorescence and is independent of spatial coordinate or spatial frequency. It should be noted that by nature of the Fourier transform, the r-space diffuse component, a_{Dn}, and the corresponding k-space form, $\tilde{a}_{Dn}$, exhibit precisely opposite temporal behavior. We will show below using simulations that while the $\tilde{a}_D$ decays at a faster rate with increasing spatial frequency, the decay rate of $\tilde{a}_F$ is independent of time. In other words, the diffusive term can be suppressed compared to the fluorescence term at higher spatial frequencies, thereby allowing the direct detection of short fluorescence lifetimes from the decay of the time-resolved diffuse fluorescence signal.

3. SIMULATIONS

We next present simulations to validate the time-resolved fluorescence signal calculated using complex integration and to illustrate the key implications of the final expressions, Eqs. (5) and (10). Consider an infinite slab diffusive medium of thickness 2 cm, with homogeneous absorption and scattering ($\mu_a = 0.1$/cm and $\mu_s = 10$/cm), and a source and detector located in the $z = 0$ and $z = 2$ cm planes, respectively (we ignore boundary conditions for the present discussion, as they do not affect the main conclusions of the paper). A 1 mm^3 fluorescent inclusion is located in between the source and detector at a distance of $z = 1$ cm from both. All computations were performed in MATLAB (The Mathworks Inc.). The Cauchy principal value integral was calculated using the function cpv.m from MATLAB central. Figure 2 shows the TD fluorescence signal calculated using the full expression in Eq. (1) (solid line) compared with Eq. (5), calculated using complex integration (filled circles). The excellent agreement between the analytical and exact time-resolved fluorescence signal [given by Eq. (1)] is clear when the lifetime is either longer ($\tau = 1$ ns) or shorter ($\tau = 0.3$ ns) than the intrinsic absorption timescale ($\tau_a = (v\mu_a)^{-1} \approx 0.47$ ns). While the complex analysis agrees

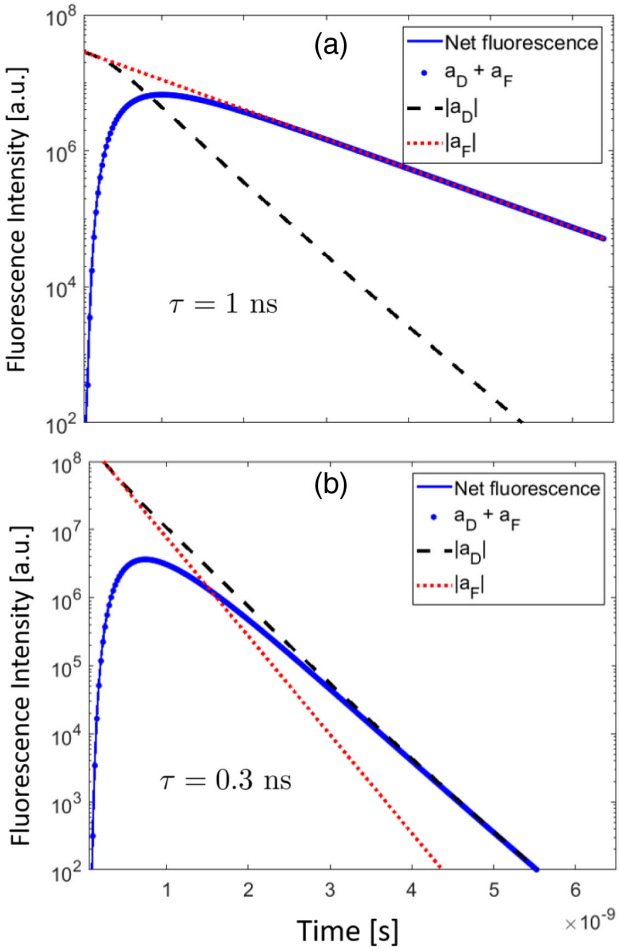

Fig. 2. Comparison of time-resolved fluorescence calculated using the exact expressions [Eq. (1), solid blue] and using complex integration [Eqs. (5)–(8), filled circles] from a 1 mm^3 fluorescent inclusion at the center of a 2 cm thick diffusive slab ($\mu_a = 0.1$/cm and $\mu_s = 10$/cm), for a single source and detector located at the $z = 0$ and $z = 2$ cm planes. The lifetime of the inclusion is either (a) $\tau = 1$ ns or (b) 0.3 ns, which are, respectively, longer and shorter compared to the intrinsic absorption timescale of $1/(v\mu_a) \approx 0.47$ ns. The calculation using complex analysis [Eq. (5) in the text, blue filled circles] and using the full TD in the adjoint formulation [Eq. (1) solid blue] are shown. The diffusive (dashed line, black) and fluorescent (dotted line, red) contributions to the net time-resolved fluorescence signal, as calculated by the complex analysis treatment, are also shown.

well with the exact time-resolved fluorescence signal, it also delineates the signal into diffusive (black dashed line) and fluorescent (red dotted line) components. The net time-resolved fluorescence signal asymptotically approaches the fluorescent decay term for $\tau = 1$ ns, and approaches the diffusive term when $\tau = 0.3$ ns, which is as expected, since the intrinsic fluorescent decay dominates the long time behavior of the diffuse time-resolved fluorescence for long lifetimes. Further, the asymptotic decay time of the time-resolved fluorescence signal is dominated by τ_a when $\tau < \tau_a$, which therefore precludes a direct measurement of the intrinsic fluorescence lifetime of a fluorophore embedded in a diffuse medium. We will see below that the use of higher spatial frequencies allows the direct detection of the true intrinsic lifetime even when $\tau < \tau_a$.

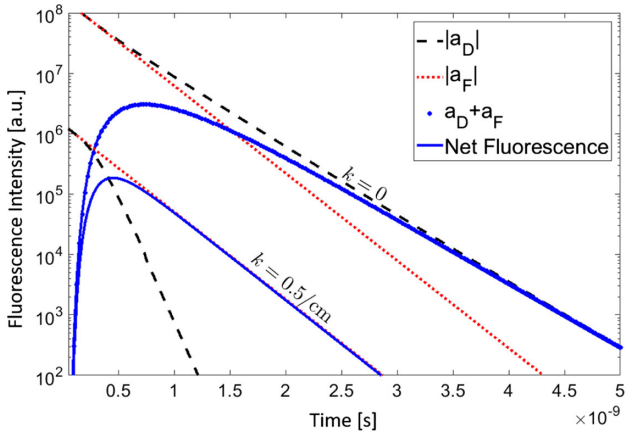

Fig. 3. Comparison of time-resolved fluorescence for the same geometry as in Fig. 2, but for spatial-frequency domain excitation and detection (instead of point sources) in the planes $z = 0$ and $z = 2$ cm. The net TD fluorescence calculated using complex analysis (filled circle) and the full TD expression (solid blue) are shown for source and detector spatial frequencies of $k_s = k_d = 0$ and $k_s = k_d = 0.5$ cm^{-1}. The corresponding diffusive [$\tilde{a}_D$, Eq. (12), black dashed line] and fluorescent [$\tilde{a}_F$, Eq. (11), dotted red line] contributions are shown as for $k_s = k_d = 0$ and $k_s = k_d = 0.5$ cm^{-1}.

We next compare the SFD expressions for the full TD signal [Eqs. (9) and (1)] and the results from complex integration [Eq. (10)]. Figure 3 shows the time-resolved fluorescence signal calculated using Eq. (10) (solid blue) compared with the FFT of the exact expression calculated using Eqs. (9) and (1) (filled circles), for the same geometry as in Fig. 2 but with an inclusion lifetime of $\tau = 0.3$ ns, which is shorter than the intrinsic absorption timescale (0.47 ns). Shown are the simulations for two spatial frequencies, namely, $k = 0$ (i.e., uniform, wide-field excitation) and $k = 0.5$ cm^{-1}, where k is the absolute magnitude of the source and detector spatial frequencies, which were set to be equal ($|\mathbf{k}_s| = |\mathbf{k}_d| = k$). Also shown are the corresponding diffusive [$\tilde{a}_{Dn}$, black, Eq. (12)] and pure fluorescent decay [$\tilde{a}_{Fn}$, red, Eq. (11)] amplitudes. The excellent agreement between the full TD expression and the complex analytical calculation once again confirms the validity of the derivation above. We note that for the $k = 0$ case, the net fluorescence decay approaches the diffusive component a_D, which is expected since the lifetime is shorter than the intrinsic absorption timescale. However, at the higher spatial frequency of $k = 0.5$ cm^{-1}, the net fluorescence approaches the pure fluorescence decay component, while the decay rate of a_D (slope of the dashed black line in Fig. 3) is much higher than that for $k = 0$. Thus, the diffuse component is more rapidly attenuated at high spatial frequencies, while the rate of attenuation of the fluorescence decay (slope of the red dotted line in Fig. 3) is independent of spatial frequency. The behavior of the diffuse component is analogous to that of the decay of intrinsic diffuse light, which has been shown to decay at a faster rate at higher spatial frequencies [4]. To further illustrate the difference between the diffuse and fluorescent contributions in k space, we plot the spatial frequency dependence of a_D and a_F over a wider range of k values, for two time points along the asymptotic decay portion of the TD fluorescence signal (Fig. 4).

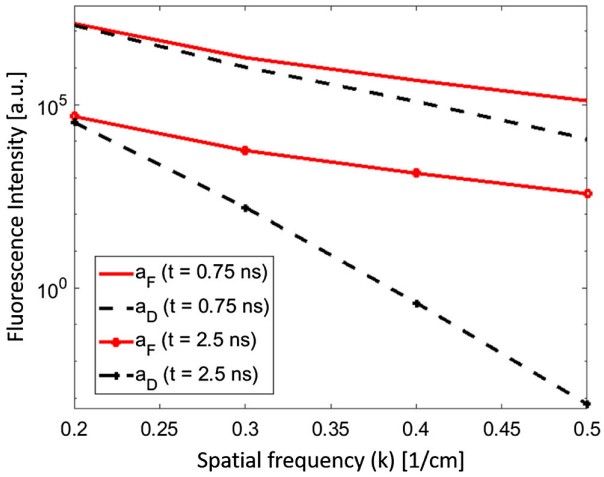

Fig. 4. Spatial-frequency dependence of the diffusive ($\tilde{a}_D$, black line) and fluorescent ($\tilde{a}_F$, red line) contributions to the time-resolved diffuse fluorescence at two time points (0. 75 ns, solid line, and 2.5 ns, dashed line) in the asymptotic (decay) portion of the signal.

The spatial frequencies were chosen to be equal for all components and for the source and detector, i.e., $|\mathbf{k}_s| = |\mathbf{k}_d| = k$. It is clear that the spatial frequency dependence of the diffuse component is strongly dependent on time, whereas the slope of the fluorescent decay amplitude does not depend on time. At high spatial frequencies and long times, the diffusive component is several orders of magnitude smaller than the fluorescence amplitude, explaining the approach of the net fluorescence towards the intrinsic fluorescence decay at high spatial frequencies. Figures 3 and 4 together illustrate the important advantage of the use of high spatial frequencies for eliminating the intrinsic diffusive component of diffuse fluorescence signals, which allows the detection of lifetimes shorter than the intrinsic absorption timescale.

4. DISCUSSION AND CONCLUSION

We have presented a complete derivation of time-resolved fluorescence propagation in a turbid medium obeying the diffusion equation using complex analytical methods. The analysis shows that the intrinsic absorption timescale, $\tau_a = v(\mu_a)^{-1}$, plays an important role in the temporal evolution of diffuse fluorescence signal: the signal takes two distinct forms depending on the relative value of the fluorescence lifetimes, τ_n, with respect to τ_a. We derive expressions for both cases using complex integration, which shows that time-resolved diffuse fluorescence can be written as a sum of purely diffusive and purely fluorescent decay components that exhibit distinct spatiotemporal responses. These components arise from distinct features in the complex plane, namely, branch points, located at $-i/\tau_a$ and simple pole singularities, located at $-i/\tau_n$. In the space–time domain, the diffusive term behaves analogous to the intrinsic (non-fluorescent) diffuse light [1], exhibiting a spatial broadening with time, while the fluorescent term is factorized into a product of space and time factors, exhibiting a spatial distribution with a width that remains constant in time.

We have also presented the corresponding expressions for the time-resolved fluorescence signal in SFD, where point sources and detectors are replaced with spatially harmonic excitation and detection patterns. Once again, the diffuse time-resolved fluorescence signal takes a distinct form depending on whether the value of the fluorescence lifetime is greater or less than the intrinsic absorption timescale. The spatial and temporal evolutions are mixed in the diffuse term, such that higher spatial frequencies decay at a faster rate than the low spatial frequencies, corresponding to a narrowing of the k-space distributions with time. On the other hand, the spatial and temporal terms are completely factorized in the fluorescence term, which thus exhibits a spatial or spatial-frequency distribution that is independent of time except for a uniform decay at the characteristic lifetime(s) of the fluorophore(s) embedded in the turbid medium. Thus, at high spatial frequencies and long times, the intrinsic fluorescence decay term dominates the net diffuse fluorescence signal. We have previously shown experimentally that this phenomenon can be exploited by employing high spatial frequencies to detect short fluorescence lifetimes in turbid media [11,17]. The present work provides a theoretical derivation that explains this phenomenon, using a complex analytical treatment of the time-resolved diffuse fluorescence signal expressed in FD. The analysis shows that a single timescale, namely, τ_a, determines the asymptotic or long time behavior of fluorescence in diffuse media. Thus, it is possible to recover the intrinsic fluorescence lifetime from absorbing and scattering tissue for both cases when the lifetimes are shorter or longer than τ_a. While we have demonstrated this effect experimentally before, this paper presents a theoretical basis for the previous experimental results, using new expressions derived for short lifetimes and for spatially modulated sources. To our knowledge, this paper presents the first treatment of time-resolved diffuse fluorescence using complex analysis, which results in semi-analytical expressions that also provide physical insights into the spatiotemporal behavior of fluorescence in diffuse media. While this paper is focused on the behavior of fluorescence in a diffuse medium, this is also the first analysis, to our knowledge, to discuss the complex plane structure of the diffuse Green's function. The analysis presented herein could therefore have relevance for modeling the more general case of non-fluorescent light propagation in diffuse media for various biomedical applications [3].

Funding. National Cancer Institute (R01-CA-211084).

Disclosures. The author has no conflicts of interests to disclose.

REFERENCES

1. M. S. Patterson, B. Chance, and B. C. Wilson, "Time resolved reflectance and transmittance for the noninvasive measurement of tissue optical properties," Appl. Opt. **28**, 2331–2336 (1989).
2. J. C. Haselgrove, J. C. Schotland, and J. S. Leigh, "Long-time behavior of photon diffusion in an absorbing medium: application to time-resolved spectroscopy," Appl. Opt. **31**, 2678–2683 (1992).
3. S. R. Arridge and J. C. Schotland, "Optical tomography: forward and inverse problems," Inverse Prob. **25**, 123010 (2009).
4. A. Bassi, C. D'Andrea, G. Valentini, R. Cubeddu, and S. Arridge, "Temporal propagation of spatial information in turbid media," Opt. Lett. **33**, 2836–2838 (2008).

5. D. J. Cuccia, F. Bevilacqua, A. J. Durkin, and B. J. Tromberg, "Modulated imaging: quantitative analysis and tomography of turbid media in the spatial-frequency domain," Opt. Lett. **30**, 1354–1356 (2005).
6. D. J. Cuccia, F. Bevilacqua, A. J. Durkin, F. R. Ayers, and B. J. Tromberg, "Quantitation and mapping of tissue optical properties using modulated imaging," J. Biomed. Opt. **14**, 024012 (2009).
7. V. Lukic, V. A. Markel, and J. C. Schotland, "Optical tomography with structured illumination," Opt. Lett. **34**, 983–985 (2009).
8. A. Mazhar, D. J. Cuccia, S. Gioux, A. J. Durkin, J. V. Frangioni, and B. J. Tromberg, "Structured illumination enhances resolution and contrast in thick tissue fluorescence imaging," J. Biomed. Opt. **15**, 010506 (2010).
9. V. Venugopal, J. Chen, F. Lesage, and X. Intes, "Full-field time-resolved fluorescence tomography of small animals," Opt. Lett. **35**, 3189–3191 (2010).
10. N. Ducros, A. Bassi, G. Valentini, G. Canti, S. Arridge, and C. D'Andrea, "Fluorescence molecular tomography of an animal model using structured light rotating view acquisition," J. Biomed. Opt. **18**, 20503 (2013).
11. A. T. N. Kumar, "Fluorescence lifetime detection in turbid media using spatial frequency domain filtering of time domain measurements," Opt. Lett. **38**, 1440–1442 (2013).
12. M. A. Oleary, D. A. Boas, X. D. Li, B. Chance, and A. G. Yodh, "Fluorescence lifetime imaging in turbid media," Opt. Lett. **21**, 158–160 (1996).
13. J. Mathews and R. L. Walker, *Mathematical Methods of Physics* (WA Benjamin, 1970), Vol. **501**.
14. T. Durduran, A. Yodh, B. Chance, and D. Boas, "Does the photon-diffusion coefficient depend on absorption?" J. Opt. Soc. Am. A **14**, 3358–3365 (1997).
15. K. E. Oughstun and G. C. Sherman, "Uniform asymptotic description of electromagnetic pulse propagation in a linear dispersive medium with absorption (the Lorentz medium)," J. Opt. Soc. Am. A **6**, 1394–1420 (1989).
16. A. T. Kumar, S. B. Raymond, G. Boverman, D. A. Boas, and B. J. Bacskai, "Time resolved fluorescence tomography of turbid media based on lifetime contrast," Opt. Express **14**, 12255–12270 (2006).
17. A. T. Kumar, S. S. Hou, and W. L. Rice, "Tomographic fluorescence lifetime multiplexing in the spatial frequency domain," Optica **5**, 624–627 (2018).